Fusion of MODIS-MISR aerosol inversion for estimation of aerosol absorption

Eric F. Vermote [a,b,*], Jean-Claude Roger [a,c,d], Alexander Sinyuk [c,e], Nazmi Saleous [b,f], Oleg Dubovik [c]

[a] *University of Maryland, Department of Geography, United States*
[b] *NASA/GSFC Code 614.5, United States*
[c] *NASA/GSFC Code 614.4, United States*
[d] *ELICO, Université du Littoral Côte d'Opale, France*
[e] *SSAI, United States*
[f] *SAIC, United States*

Abstract

This paper presents an approach for estimating aerosol absorption by combining MODIS and MISR data. The approach uses a previously published concept based on combining clear and hazy days to retrieve aerosol absorption. It augments the existing approach by using multi-sensor data to improve the surface characterization and aerosol property retrieval. MODIS data are used to retrieve the aerosol optical thickness, whereas MISR data are first used to determine the surface properties on the clear day, and then to retrieve aerosol absorption on hazy days by using the derived surface properties as the ground boundary condition. The method is applied to two extreme cases of absorption in biomass burning situations: One case over Mongu (South Africa) and the other over Alta Floresta (Brazil). The range of single scattering albedo retrieved values is from 0.7 to 0.95. A comparison with AERONET independent estimates shows very good agreement (better than 0.02 on average) across the whole range.
© 2007 Elsevier Inc. All rights reserved.

1. Introduction

The effect of aerosol on climate depends on its optical properties (absorption and scattering) (Fraser & Kaufman, 1985; Satheesh & Ramanathan, 2000). Low absorption leads to top of atmosphere cooling, while heating can take place inside the atmosphere for strong absorption (Hansen et al., 1997; IPCC, 2001).

To estimate the aerosol global impact on the climate system, we need to know the global repartition of the absorption (or of the single scattering albedo ω_o). Though derivation of an aerosol absorption climatology from ground-based networks is possible (Dubovik et al., 2002; Schuster et al., 2005), satellite retrieval is one of the most useful tools to comprehend global aerosol absorption (Kaufman et al., 2002a,b). Kaufman (1987), for example, used Landsat measurements to derive the single scattering albedo of aerosol from a forest fire transported over the Washington D.C. region. Kaufman et al. (1990) reported a method to infer absorption by analyzing a pair of AVHRR images. Other studies take advantage of the effect of the absorption over bright desert surfaces, using Landsat (Kaufman et al., 2001) or MODIS (Hsu et al., 2004; Satheesh & Srinivasan, 2005). In the same manner, Kaufman et al. (2002a) proposes a new measurement strategy for the assessment of aerosol absorption using polarimetric measurements from space over oceanic sunglint regions. Recently, Torres et al. (2005) proposes a method to retrieve aerosol absorption from TOMS observations in the near UV.

Aerosol absorption occurs when dust and/or black carbon kernels are present in the aerosol particle. Even if dust events lead to an important climatic effect (Prospero et al., 2002; Tanré et al., 2003), the carbonaceous aerosol remains the main

* Corresponding author. University of Maryland, Department of Geography, United States.
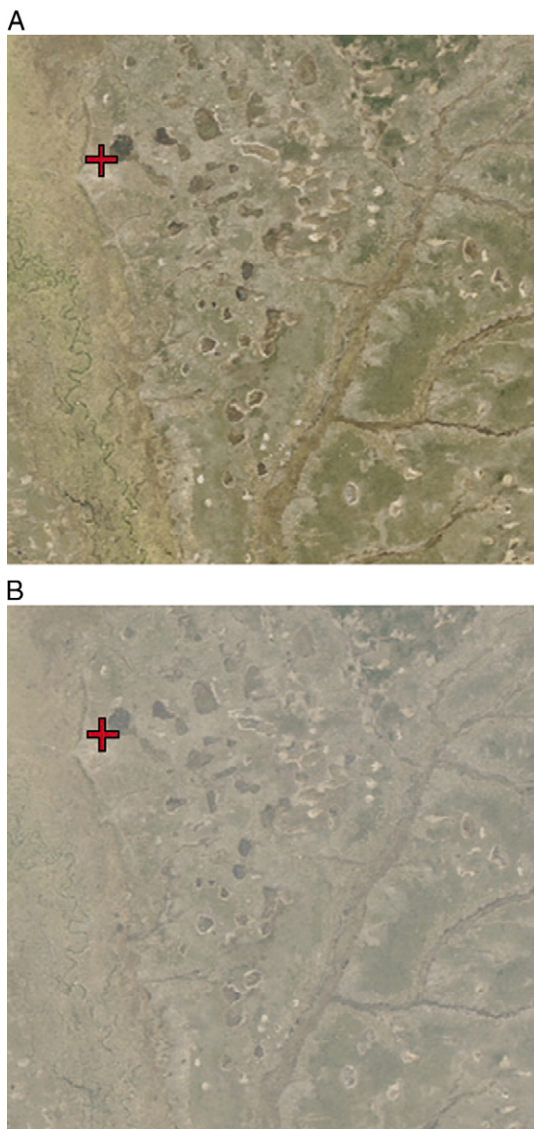*E-mail address:* eric@ltdri.org (E.F. Vermote).

In this paper, we propose to characterize aerosol absorption for biomass burning smoke by inverting the single scattering albedo for a Savanna case (Mongu area in Zambia) and for a forest case (Alta Floresta area in Brazil). For that purpose, we use a pair of MISR (Diner et al., 1998) images and a pair of MODIS images acquired on a clear and a hazy day. MODIS data are used to derive the aerosol optical thickness using the extended dark target approach (Remer et al., 2005). MISR data are used in the clear days to characterize the surface properties in the red and near-infrared bands. The derived surface properties are used as ground boundary conditions to invert the aerosol absorption for hazy days where the aerosol optical thickness is retrieved from MODIS data and the size distribution

Fig. 1. A and B: RGB image of the area near Mongu AERONET site (15.25 degree South, 23.15 degree East), for the clear day -1a- (July, 17, 2004, path 176 orbit 24363) and for the hazy day -1B- (August, 2, 2004, path 176, orbit 24596). The data have been corrected for the molecular scattering effect. The location of the test site used in the analysis (3 km × 3 km) is indicated by a red cross.

important actor in the aerosol absorbing processes (Haywood & Ramaswamy, 1998; Jacobson, 2002; Myhre et al., 1998; Penner et al., 1998, 2003; Ramanathan et al., 2001). In these processes, smoke from biomass burning can generate a strong local impact (Hobbs et al., 1997; Penner et al., 1992; Ramanathan et al., 2001). For that case, there are two different combustibles for fires: savanna and forest, yielding two different burning processes. Savanna burns quickly with a strong flaming stage emitting a large quantity of black carbon. Forest fires emit smoke, first during a flaming stage with an emission of black carbon, and then during a long smoldering stage dominated by fine organic particles. According to Kaufman et al. (2002a,b), 12% of the African savanna smoke aerosol optical thickness (AOT) is due to absorption of black carbon while the fraction is only 7% for the forest fire smoke.
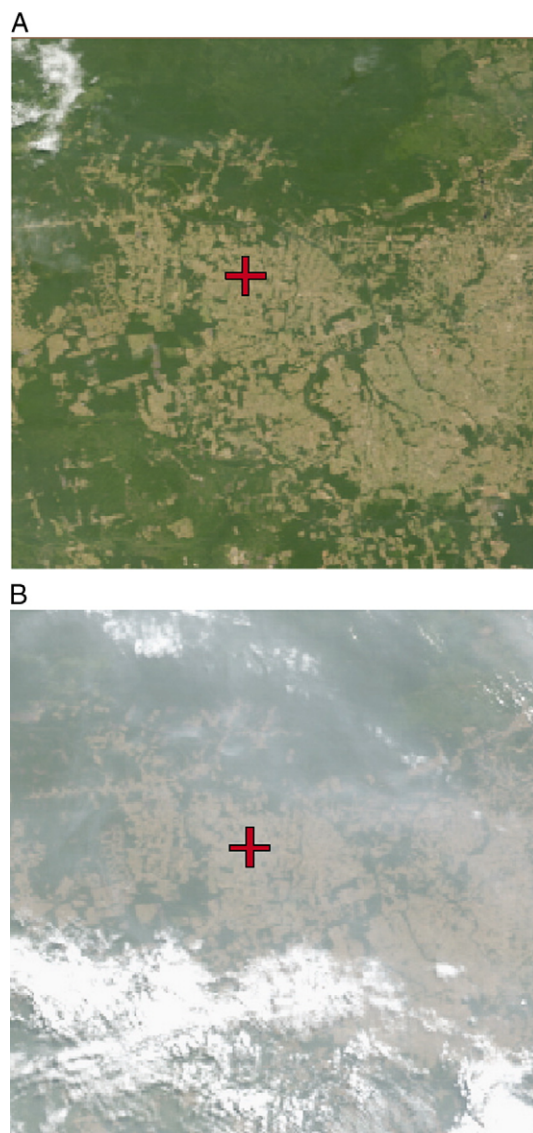
Fig. 2. A and B: RGB image of the area near the Alta Floresta AERONET site (9.92 degree South, 56.02 degree West), for the clear day -2A- (July, 22, 2004, path 227, orbit 24439), and for the hazy day -2B- (August, 23, 2004, path 277, orbit 24905). The data have been corrected for the molecular scattering effect. The location of the test site used in the analysis (3 km × 3 km) is indicated by a red cross.

Table 1
Summary the atmospheric conditions and the ancillary data for the four cases studied

Case	Aerosol Optical depth at 0.55 μm AERONET (MODIS for the clear day)	Angstrom parameter AERONET	Ozone content [cm atm] NCEP	Water content [g/cm^2] MODIS	Solar zenith angle	View zenith angle MODIS	Relative azimuth MODIS
Mongu 7/17/2004 08h50GMT	0.155 (0.21)	1.85	0.273	1.11	43.86	13.40	116.9
Mongu 8/2/2004 08h50GMT	0.428	1.85	0.278	1.42	41.11	13.40	118.11
Alta Floresta 7/22/2004 14h05GMT	0.116 (0.09)	1.7	0.2675	3.48	39.34	1.73	49.93
Alta Floresta 8/23/2004 14h05GMT	0.972	2.05	0.2675	4.13	32.56	1.73	40.95

and real part of the refractive index are obtained from AERONET measurements.

2. Methodology

The underlying principle of the present approach has been utilized in several methods aimed at characterizing aerosol properties from space. It relies on using a pair of images of the same area acquired under drastically different atmospheric conditions representing a "clear" and a "hazy" situation. On the "clear" day, the surface properties could be retrieved with good accuracy. On the "hazy" day, surface properties derived on the clear day could be used as ground boundary conditions and the top of the atmosphere signal could be inverted to derive aerosol properties. The originality of this method, which takes advantages of the multi-viewing capabilities of MISR, lies in the fact that the directional properties of the surface are utilized in two ways. First, they are used in better predicting the surface

contribution in the "hazy" case which is not acquired under the same geometry as the "clear" case. Secondly, they are used in better constraining the aerosol properties inversion, which is not restricted to only one view direction.

The method assumes that the surface does not vary substantially between the two selected dates. This restricts the interval of time between acquisitions depending on the season and land cover. For example, it is possible to characterize the surface once and for all over desert where the surface is generally stable (Hsu et al., 2004). Over vegetated land surfaces, phenology and potential rapid changes in land cover, such as biomass burning and deforestation restrict the maximum interval of time between two observations depending on the season. If no rapid change occurs, it is generally accepted that during a 16-day interval the surface properties can be assumed constant (Huete et al., 2002; Schaaf et al., 2002) within the error bars of the derivation (5% relative on the albedo, or 0.005 absolute or 5% relative of the spectral reflectances).
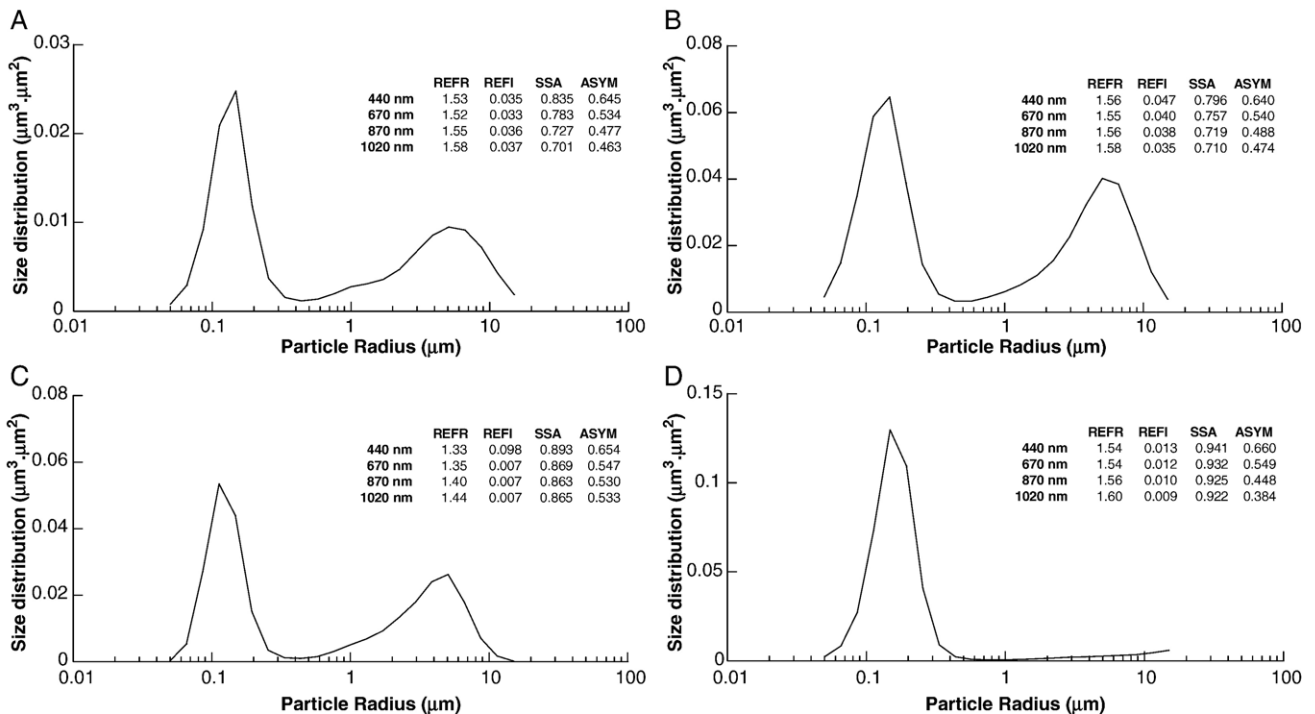

Fig. 3. A: Inversion of the aerosol characteristics on Mongu for July 17, 2004. B: Inversion of the aerosol characteristics on Mongu for August 2, 2004. C: Alta Floresta aerosol properties inverted on July 22, 2004. D: Alta Floresta aerosol properties inverted on August 23, 2004.
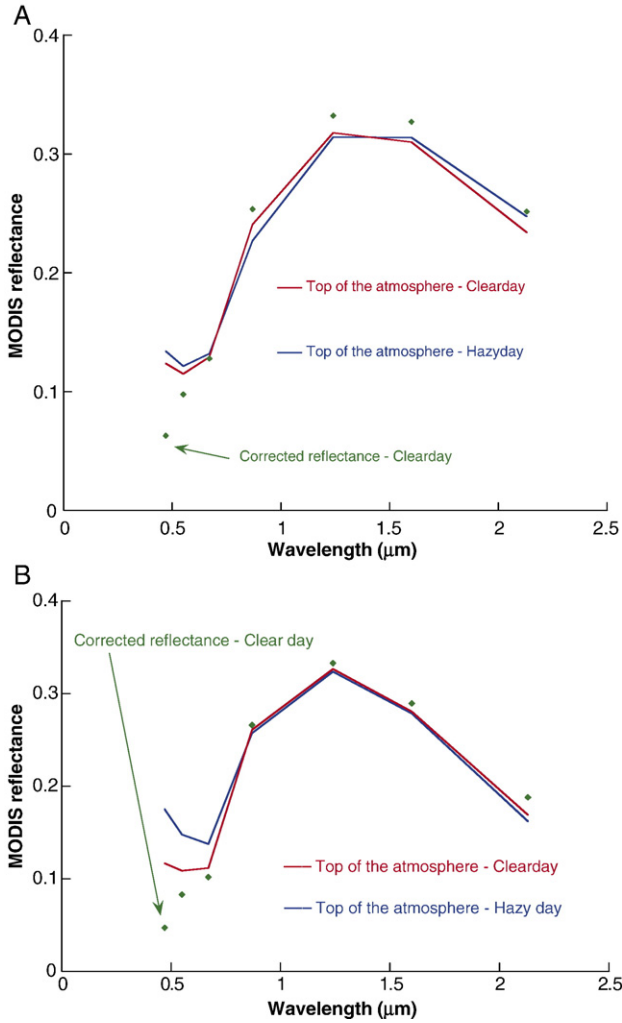
Fig. 4. A: MODIS reflectances over Mongu. B: MODIS reflectances over Alta Floresta.
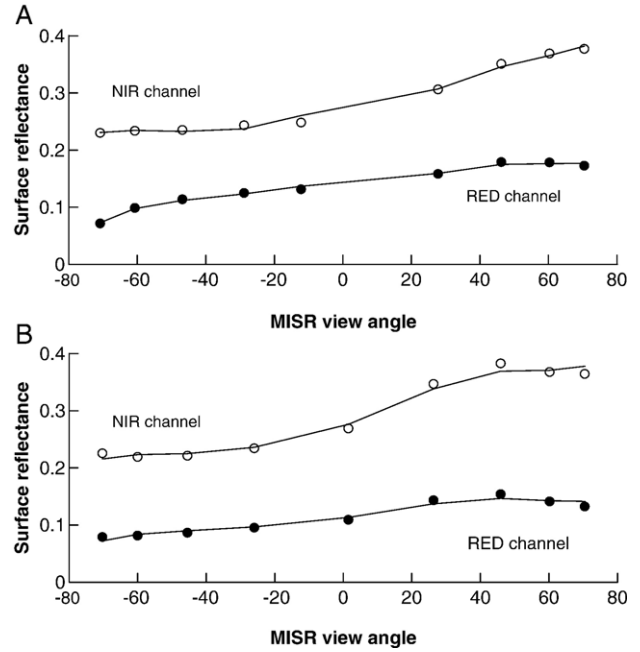

Fig. 5. A: MISR data corrected using the derived MODIS optical depth over Mongu for the clear day (the line is the BRDF model inversion). The negative (resp. positive) view angles corresponds to the backward (resp. forward) cameras. B: MISR data corrected using the derived MODIS optical depth over Alta Floresta for the clear day (the line is the BRDF model inversion). The negative (resp. positive) view angles corresponds to the backward (resp. forward) cameras.

effect as a function of the size distribution and refractive indices (assuming the Mie theory is applicable). In the present study, we focus on the feasibility of a retrieval technique of aerosol

The second difficulty in the dual date approach lies in the selection of the clear case. Without a priori knowledge of the optical thickness, some authors use a compositing technique to select data where the aerosol effect is minimal. For example, Hsu et al. (2004) use the minimum reflectivity compositing technique over desert targets and Holben et al. (1992) use the maximum contrast criterion. In our approach, we use the optical thickness derived from MODIS by the extended dark target method (Remer et al., 2005) as our "clear" case selection criterion. Despite inherent limitations of this technique for a fine determination of aerosol properties, it proves suitable for our purpose. An example of the limitations is the fact that only the blue channel can be used over bright targets and therefore the aerosol model has to be assumed. The validation of the derived optical thickness and the analysis of the derived surface properties show that in "clear" cases the surface reflectance can be derived with a relative error of 5% in the red and near infrared, and in hazy conditions the optical thickness can be derived within 20% at 0.55 μm.

Finally, the third difficulty which is related to the aerosol retrieval problem in general, is the variability of the aerosol
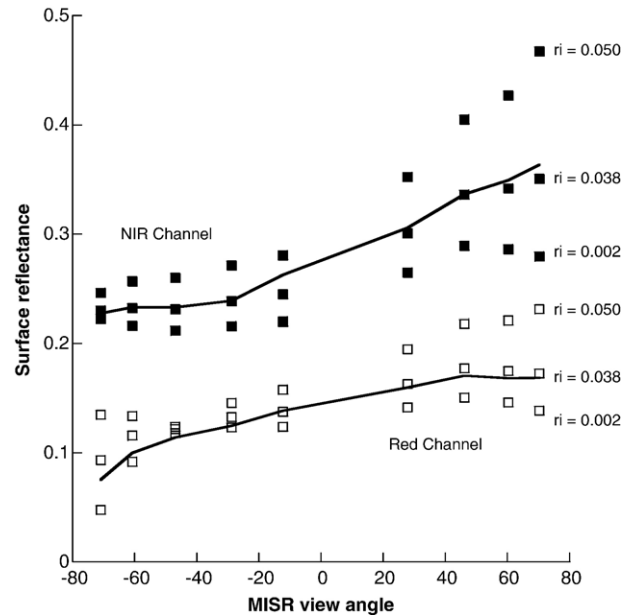

Fig. 6. Surface reflectance over the Mongu site on the hazy day (squares) and the predicted reflectance obtained using the BRDF characterized on the clear day (line) for several imaginary parts of the refractive index and for the NIR (top) and the Red (bottom) channels. The negative (resp. positive) view angles corresponds to the backward (resp. forward) cameras.
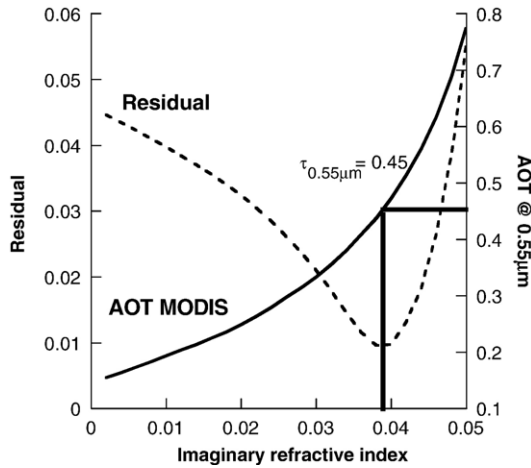
Fig. 7. Aerosol optical thickness and residual between observed and predicted reflectance's as a function of the imaginary part of the refractive index.

Fig. 9. Same as Fig. 7 but for Alta Floresta.

absorption. The absorption is parameterized by the imaginary part of the refractive index, which is the parameter we invert in our technique assuming it is not dependent on the wavelength. Once the imaginary part of the refractive index is retrieved, we can compute the spectral single scattering albedo which is directly connected to the absorption at each wavelength.

To reduce the uncertainties due to the variability of aerosol effect, we will use the aerosol size distribution and the real part of the refractive index derived from AERONET sun-photometer observations (Dubovik et al., 2002; Holben et al., 1998) leaving the absorption as a variable parameter.

Our retrieval method uses acquisitions from two dates, one "clear" and one "hazy", and is summarized by the following steps:

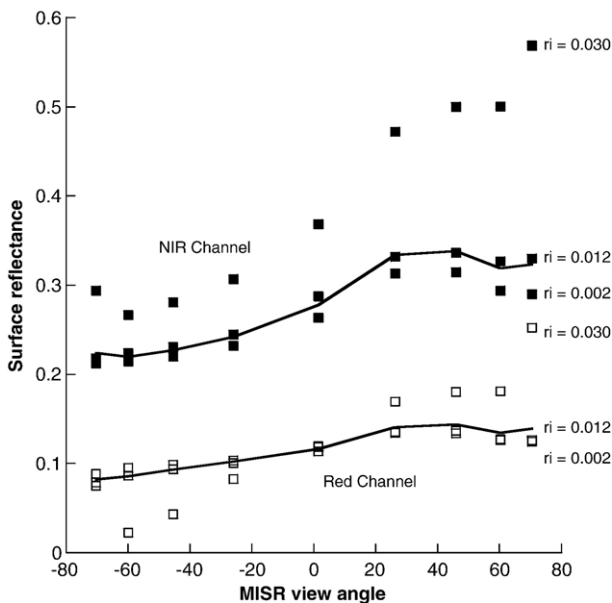(1) For the clear day, using the optical thickness derived for MODIS extended dark target method, the atmospheric

correction of MISR data in the red (0.678 μm) and the near-infrared (0.87 μm) is performed. The values of the directional reflectance in MISR's 9 cameras are used to determine the three coefficients of the MODIS operational BRDF model (Isotropic, RossThick, LiSparse Reciprocal, Schaaf et al., 2002).

(2) For the hazy day, using once again the MODIS optical thickness, the atmospheric correction of MISR data is performed for different values of the imaginary refractive index. MISR corrected reflectances are compared with the predictions from the BRDF model derived in step (1). The imaginary part of the refractive index is determined by minimizing the difference between predicted and corrected reflectances in the MISR's 9 cameras.

Fig. 8. Same as Fig. 6 but for Alta Floresta.

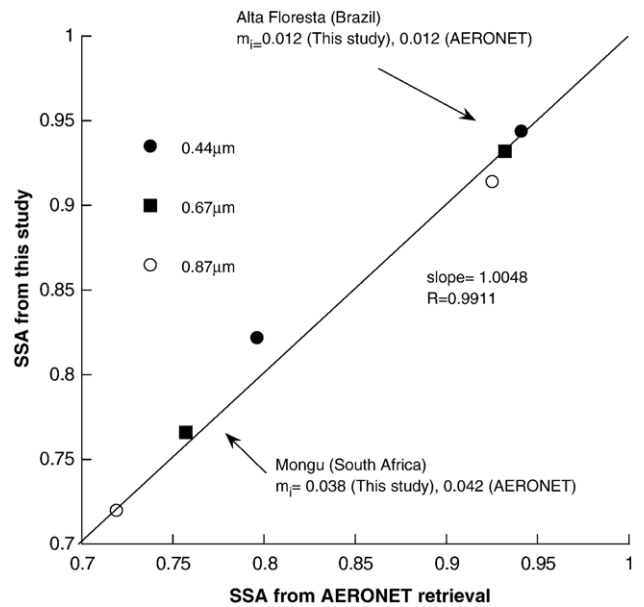Fig. 10. Comparison of the single scattering albedo at 0.44 μm, 0.67 μm and 0.87 μm with the one derived from AERONET measurements for both sites. The imaginary part of the refractive index retrieved in this study is compared to the averaged imaginary part retrieved by AERONET.

Table 2
Main characteristics of the aerosol model used in the inversion (from Dubovik et al., 2002)

Model name	AERONET data sources	Small mode radius [μm] Standard deviation	Coarse mode radius Standard deviation	Small mode volume [μm³/μm²]	Coarse mode volume [μm³/μm²]	Refractive index Real part
Smoke low absorption	Amazonian forest Brazil (1993–1994); Bolivia (1998–1999)	$0.14+0.013\tau_{0.44\ \mu m}$ 0.40	$3.27+0.58\tau_{0.44\ \mu m}$ 0.79	$0.12\tau_{0.44\ \mu m}$	$0.05\tau_{0.44\ \mu m}$	1.47
Smoke high absorption	African savanna Zambia (1995–2000)	$0.12+0.025\tau_{0.44\ \mu m}$ 0.40	$3.22+0.71\tau_{0.44\ \mu m}$ 0.73	$0.12\tau_{0.44\ \mu m}$	$0.09\tau_{0.44\ \mu m}$	1.51
Urban clean	GSFC, Greenbelt, MD (1993–2000)	$0.12+0.11\tau_{0.44\ \mu m}$ 0.38	$3.03+0.49\tau_{0.44\ \mu m}$ 0.75	$0.15\tau_{0.44\ \mu m}$	$0.01+0.04\tau_{0.44\ \mu m}$	$1.41-0.03\tau_{0.44\ \mu m}$
Urban polluted	Creteil-Paris, France (1999)	$0.11+0.13\tau_{0.44\ \mu m}$ 0.43	$2.76+0.48\tau_{0.44\ \mu m}$ 0.79	$0.01+012\ \tau_{0.44\ \mu m}$	$0.01+0.05\ \tau_{0.44\ \mu m}$	1.40
Dust	Solar Village, Saudi Arabia (1998–2000)	0.12 0.40	2.32 0.60	$0.02+002\tau_{1.02\ \mu m}$	$-0.02+0.98\tau_{1.02\ \mu m}$	1.56

To demonstrate the feasibility of this technique we study aerosols from biomass burning. Even though these aerosols generally have similar size distribution and the real part of refractive indices, they show considerable variability in absorption depending on the type of combustion and fuel burned (Dubovik et al., 2002).

3. Data set

Figs. 1A–B and 2A–B show the RGB images of the two sites selected for this feasibility study using MODIS data. The first one (Fig. 1A–B) is located over the Mongu area in Zambia. This site is representative of African savanna. The second site, Alta Floresta (Fig. 2A–B), is a typical site of the Amazonian forest in Brazil. The two sites of 3 km × 3 km were selected over relatively uniform area within 5 km of the sunphotometer location.

Table 1 summarizes the atmospheric conditions and the ancillary data for the four cases studied. Despite the relatively close Angstrom parameters, the aerosol models are quite different in terms of size distribution and absorption as illustrated by the AERONET aerosol characteristics inversion closest to the MODIS acquisition time (Fig. 3A–D).

4. Application

4.1. Retrieval of aerosol optical thicknesses using the MODIS data on clear days

The optical thickness was retrieved on the "clear" days for both sites based on MODIS data using the extended dark target technique. In this approach, an empirical relationship is assumed between the surface reflectance in the shortwave infrared (2.13 μm or band 7 of MODIS) and the blue (0.47 μm) or red wavelength (0.67 μm). The aerosol model has to be assumed in this approach (Remer et al., 2005). In this case, we simply consider that the blue channel reflectance should be 1/4 of the shortwave infrared channel. Fig. 4A–B show for each case the reflectance measured by MODIS at the top of atmosphere as well as the surface reflectance derived using the optical thickness computed from the previously described approach for the clear day. The values of AOT at 0.55 μm derived from MODIS data for the clear cases over Mongu (0.21) and Alta

Floresta (0.09) are reported in Table 1 along with the values measured by the sun-photometer (0.155 for Mongu and 0.116 for Alta Floresta). These aerosol optical depths are within the expected error bars (Remer et al., 2005). In this case, since the aerosol model is directly derived from the sun-photometer, we can safely assume that the uncertainty in the SWIR-Visible surface reflectance relationship is responsible for most of the error. This source of error has less impact with higher aerosol optical thicknesses and will lead to a decrease in the relative error when inverting the aerosol properties for the "hazy" days.

4.2. Atmospheric correction of the MISR data on the clear days

Using the MODIS optical thickness derived on the clear days together with the aerosol model measured by AERONET, we perform atmospheric correction of MISR data in the red and NIR for the nine cameras over an array of 3×3 (1 km) pixels co-

Table 3
Results of the inversion using the climatological models of Table 2

Model	Single scattering Albedo (0.44 μm, 0.67 μm, 0.87 μm)	Residual	Imaginary refractive index	Optical depth at 0.55 μm
(a) For Mongu				
AERONET (Fig. 3B)	0.8172, 0.7596, 0.7129	0.0123	0.0395	0.4635
Smoke low absorption	0.8286, 0.7716, 0.7149	0.0085	0.032	0.515
Smoke high absorption	0.8258, 0.7661, 0.7085	0.0130	0.0335	0.449
Urban clean	0.7950, 0.7453, 0.6960	0.0360	0.038	0.385
Urban polluted	0.8448, 0.7944, 0.7476	0.0097	0.026	0.492
Dust	0.7712, 0.7632, 0.7748	0.0389	0.014	0.294
(b) For Alta Floresta				
AERONET (Fig. 3D)	0.9415, 0.9261, 0.9111	0.011	0.0125	0.903
Smoke low absorption	0.9485, 0.9289, 9070	0.019	0.008	0.852
Smoke high absorption	0.9543, 0.9379, 0.9144	0.015	0.007	0.840
Urban clean	0.9923, 0.9911, 0.9894	0.042	0.005	1.18
Urban polluted	0.9605, 0.9486, 0.9360	0.0095	0.001	0.942
Dust	0.8023, 0.8101, 0.8288	0.106	0.009	0.002

located with the MODIS aerosol inversion. The atmospheric correction is done using the ancillary parameters (ozone, water vapor) given in Table 1 as well as the altitude of the target and estimates of surface pressure based on NCEP data. The atmospheric correction is performed using the Vectorial version of the 6S code (Kotchenova et al., 2006) available from http://6s.ltdri.org. The correction is done for a BRDF ground boundary condition and the convergence is achieved by successive iterations between the atmospheric correction and the BRDF parameters inversion, the process converges rapidly after 2 or 3 iterations. The BRDF model used is the linear kernel model (Isotropic, LiSparse Reciprocal, RossThick) used routinely in the derivation of the MODIS BRDF-Albedo product (Schaaf et al., 2002).

Fig. 5A and D show the surface reflectance derived by this process (symbols) as well as the inverted BRDF model (Lines) for the two cases. The RMSE errors for Mongu are 0.003 for Red and 0.005 for NIR. For Alta Floresta, the RMSE errors are a little higher, 0.005 and 0.008 respectively for the Red and NIR channels.

4.3. Retrieval of the aerosol optical depth and absorption on the hazy days

The process is done in two steps, first the aerosol thickness is derived from MODIS and second the optical thickness is used to correct the MISR Top of the atmosphere data to produce the surface reflectance. The aerosol model assumed in the process will influence the MODIS aerosol optical depth and the final surface reflectance. In this section, we choose to focus on the aerosol absorption, therefore the size distribution and real part of the refractive index are taken from the AERONET inversion (see Fig. 3B and D). We vary the imaginary part of the refractive index as it is the factor responsible for absorption. The imaginary part of the refractive index is assumed to be independent of the wavelength, which is a valid assumption in the visible and near-infrared parts of the spectrum.

Fig. 6 shows for Mongu the predicted reflectances, which are computed using the BRDF obtained on the clear day, in the MISR red and NIR bands (solid lines) as well as the corrected reflectances, which are obtained through atmospheric correction of the data on the hazy day, using several imaginary parts of the refractive index. For very strong absorption, $r_i = 0.05$, the corrected reflectances are both overestimated (compared to the prediction) especially in the backscattering direction (view angles ranging from $+20°$ to $+70°$). For very small absorption, $r_i = 0.002$, the corrected reflectances are underestimated. Fig. 6 also shows the final value selected for the imaginary part of the refractive index (0.038). This value was found by minimizing the difference between the predicted and corrected reflectance (residuals). Residuals are computed using the following equation:

$$\text{Residual} = \frac{\sum_{i=1}^{9} |\rho_{\text{red}_i}^{\text{cor}} - \rho_{\text{red}_i}^{\text{pred}}|}{9} + \frac{\sum_{i=1}^{9} |\rho_{\text{NIR}_i}^{\text{cor}} - \rho_{\text{NIR}_i}^{\text{pred}}|}{9} \quad (1)$$
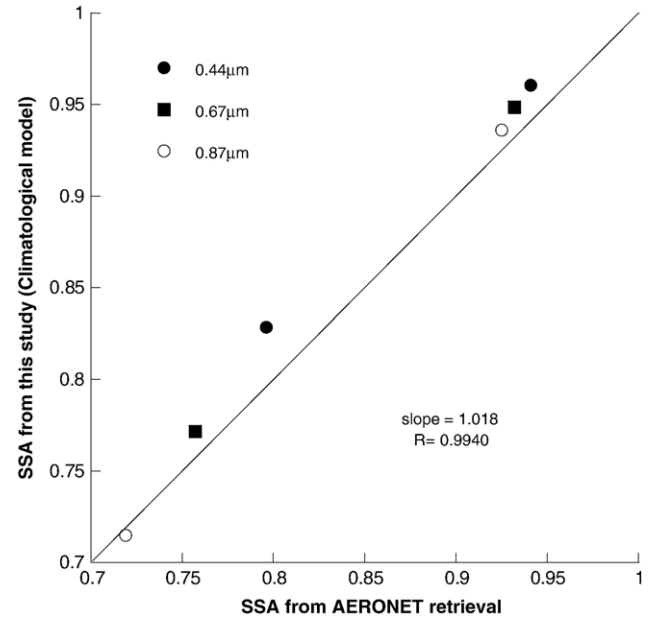

Fig. 11. Comparison of the single scattering albedo at 0.44 μm, 0.67 μm and 0.87 μm with the one derived from AERONET measurements for both sites. The results are reported for the climatological model which gives the lowest residual.

where $\rho_{\text{band}_i}^{\text{cor}}$ is the corrected reflectance in red or NIR for camera i, and $\rho_{\text{band}_i}^{\text{pred}}$ is the predicted reflectance in red or NIR for camera i.

Fig. 7 shows the variation of the residual computed using Eq. (1) as a function of the assumed imaginary part of the refractive index. It clearly shows a minimum around 0.038. It is worth noticing the variation of the aerosol optical thickness of MODIS as a function of the absorption. The value of the aerosol optical thickness increases with the absorption as the MODIS retrieval in the blue is sensitive to the aerosol path radiance which decreases as the absorption increases. For the minimum residual condition, the inverted aerosol optical depth at 0.55 μm (~ 0.45) is very close to value measured by AERONET (0.428). Over Mongu on the hazy day, the aerosol layer is rather uniform and this agreement shows that the inversion is very consistent.

The same procedure is applied to the Alta Floresta data (Fig. 8). The retrieved imaginary part of the refractive index is much lower (0.012) than for Mongu. The retrieved aerosol optical thickness at 0.55 μm (0.90) is also in good agreement with the AERONET measurements (0.972), however the aerosol layer is less uniform than that for Mongu which may explain the larger difference between the retrieval and AERONET measurement.

It is important to clarify that the same aerosol model (size distribution and imaginary and real part of the refractive index) is used for MODIS AOT retrieval and in the correction of the MISR red and near-infrared reflectances. Changing the imaginary part of the refractive index will change the MODIS retrieved AOT as well. In both Alta Floresta and Mongu cases, when the residual is minimum, not only the retrieved single scattering albedo's are close to the AERONET inversion but also the MODIS retrieved AOT is close to the AERONET measurement (Fig. 9).

5. Results and comparison to AERONET estimate of absorption

Using the aerosol model derived in Section 4 for the Hazy days over Mongu and Alta Floresta, we computed using Mie theory the aerosol single scattering albedo in the Blue (where the optical thickness is retrieved from MODIS), Red and NIR (where the imaginary part of refractive indices are retrieved from the MISR data) and compared them to the values reported by AERONET (Fig. 3B,D). The results are presented on Fig. 10. The three highest values correspond to the Alta Floresta case and the three lowest to the Mongu case. Despite the reduced number of points available for the comparison, one can see that the agreement is very good between the two estimates which cover a large range of absorption for biomass burning.

This method enables intercomparing the results of the absorption over AERONET sites, which could be of interest by itself, but in order to extend the results outside of the AERONET location, we need to use a prescribed size distribution and the real part of the refractive index. Following the approach used for MODIS aerosol retrieval over land surfaces, we have used five basics aerosol type extracted from the AERONET aerosol climatology (Dubovik et al., 2002). The characteristics of the aerosol type are summarized in Table 2. The aerosol models selected cover a range of representative type (two smoke models, two urban models and a dust model). We used those predefined models in lieu of the AERONET measured sized distribution and refractive indices on the hazy days (it is assumed that on the clear day, given the low optical thickness, a standard smoke low absorption model can be used to derive the reference BRDF).

The results are presented in Table 3a (Mongu) and b (Alta Floresta), where we give for each model and the AERONET inverted size distribution, the inverted imaginary part of the refractive index, the optical thickness, and the single scattering albedo's ($0.44\ \mu m$, $0.67\ \mu m$ and $0.87\ \mu m$). Generally, the smoke and urban polluted models give a comparable residual (between ~ 0.01 and 0.02) and despite large variation in the imaginary part of the refractive index (from 0.026 to 0.0335) a single scattering albedo within 0.02 of the AERONET retrieval. Fig. 11 shows the single scattering albedo comparison between the AERONET retrieval and the inversion for the climatological model which gives the lowest retrieval. There is a degradation of the performance compared to Fig. 10 but the accuracy is still very good (within 0.02 on average).

6. Conclusions

We have shown the feasibility of an approach for estimating the absorption of aerosol using MODIS and MISR data under specific conditions. The method in the cases investigated shows very good performance for well documented cases of absorption (biomass burning). The advantage of this method is that it can be applied at the pixel level and does not necessitate spatial uniformity of the aerosol layer which can be difficult to obtain for biomass burning cases. However, it requires temporal stability of the surface between the two acquisitions (clear and hazy days). The use of the multi-angle data from MISR enables better control of the surface influence (variation in geometry between clear and hazy day) and also improves the sensitivity to the aerosol absorption as off nadir views are more sensitive to absorption.

Although optical thickness can be derived from MISR, the use of MODIS for estimating the aerosol optical thickness was mainly justified by our familiarity with the MODIS inversion algorithm. The ability of MISR to retrieve the particle size distribution and the development of aerosol retrieval at higher spatial resolution (planned by the MISR group) justifies future investigations to use MISR by itself in retrieving the aerosol absorption using the current approach.

References

Diner, D. J., Beckert, J. C., Reilly, T. H., Bruegge, C. J., Conel, J. E., Kahn, R. A., et al. (1998). Multi-angle imaging spectroradiometer (MISR) instrument description and experiment overview. *IEEE Transactions on Geoscience and Remote Sensing, 36*, 1072−1087.

Dubovik, O., Holben, B. N., Eck, T. F., Smirnov, A., Kaufman, Y. J., King, M. D., et al. (2002). Variability of absorption and optical properties of key aerosol types observed in worldwide locations. *Journal of the Atmospheric Sciences, 59*, 590−608.

Fraser, R. S., & Kaufman, Y. (1985). The relative importance of scattering and absorption in remote sensing. *IEEE Transactions on Geoscience and Remote Sensing, 23*, 625−633.

Hansen, J., Sato, M., & Ruedy, R. (1997). Radiative forcing and climate response. *Journal of Geophysical Research, 102*, 6831−6864.

Haywood, J. M., & Ramaswamy, V. (1998). Global sensitivity studies of the direct radiative forcing due to anthropogenic sulfate and black carbon aerosols. *Journal of Geophysical Research, 103*, 6043−6058.

Hobbs, P. V., Reid, J. S., Kotchenruther, R. A., Ferek, R. J., & Weiss, R. (1997). Direct radiative forcing by smoke from biomass burning. *Science, 275*, 1776−1778.

Holben, B. N., Eck, T. F., Slutsker, I., Tanre, D., Buis, J. P., Setzer, A., et al. (1998). AERONET—A federated instrument network and data archive for aerosol characterization. *Remote Sensing of Environment, 66*(1), 1−16.

Holben, B. N., Vermote, E., Kaufman, Y. J., Tanre, D., & Kalb, V. (1992). Aerosol retrieval over land from AVHRR data-application for atmospheric correction. *IEEE Transactions on Geoscience and Remote Sensing, 30*, 212−222.

Hsu, N. C., Tsay, S. C., King, M., & Herman, J. R. (2004). Aerosol properties over bright-reflecting source regions. *IEEE Transactions on Geoscience and Remote Sensing, 42*, 557−569.

Huete, A., Didan, K., Miura, T., Rodriguez, E. P., Gao, X., & Ferreira, L. G. (2002). Overview of the radiometric and biophysical performance of the MODIS vegetation indices. *Remote Sensing of Environment, 83*, 195−213.

Intergovernmental Panel on Climate Change (2001). Climate Change 2001: The Scientific Basis. http://www.grida.no/climate/ipcc_tar/wg1/figts-22.htm

Jacobson, M. (2002). Control of fossil-fuel particulate black carbon and organic matter, possibly the most effective method of slowing global warming. *Journal of Geophysical Research, ISSN: 0148-0227, 107*(D19). doi:10.1029/2001JD001376

Kaufman, Y. J. (1987). Satellite sensing of aerosol absorption. *Journal of Geophysical Research, 92*, 4307−4317.

Kaufman, Y. J., Fraser, R. S., & Ferrare, R. A. (1990). Satellite remote sensing of large scale air pollution — Method. *Journal of Geophysical Research, 95*, 9895−9909.

Kaufman, Y. J., Martins, J. V., Remer, L. A., Schoeberl, M. R., & Yamasoe, M. A. (2002a). Satellite retrieval of aerosol absorption over the oceans using sunglint. *Geophysical Research Letters, 29*(19). doi:10.1029/2002GL015403

Kaufman, Y. J., Tanre, D., & Boucher, O. (2002b). A satellite view of aerosols in the climate system. Review. *Nature, 419*, 215−223.

Kaufman, Y. J., Tanré, D., Karnieli, A., & Remer, L. A. (2001). Absorption of sunlight by dust as inferred from satellite and ground-based remote sensing. *Geophysical Research Letters, 28*, 1479−1482.

Kotchenova, S. Y., Vermote, E. F., Matarrese, R., & Klemm, F. (2006). Validation of a new vector version of the 6S radiative transfer code for atmospheric correction of MODIS data: Part I — Path Radiance. *Applied Optics, 45*(26), 6762−6774.

Myhre, G., Stordal, F., Restad, K., & Isaksen, I. (1998). Estimates of the direct radiative forcing due to sulfate and soot aerosols. *Tellus, 50B*, 463−477.

Penner, J. E., Chuang, C. C., & Grant, K. (1998). Climate forcing by carbonaceous and sulfate aerosols. *Climate Dynamics, 14*, 839−851.

Penner, J. E., Dickinson, R. E., & O'Neill, C. A. (1992). Effects of aerosol from biomass burning on the global radiation budget. *Science, 256*, 1432−1434.

Penner, J., Zhang, S., & Chuang, C. (2003). Soot and smoke aerosol may not warm climate. *Journal of Geophysical Research, ISSN: 0148-0227, 108*(D21). doi:10.1029/2003JD003409

Prospero, J., Ginoux, P., Torres, O., Nicholson, S., & Gill, T. (2002). Environmental characterization of global sources of atmospheric soil dust identified with the nimbus 7 total ozone mapping spectrometer (TOMS) Absorbing aerosol product. *Reviews of Geophysics, ISSN: 8755-1209, 40*(1). doi:10.1029/2000RG000095

Ramanathan, V., Crutzen, P. J., Kiehl, J. T., & Rosenfeld, D. (2001). Aerosols, climate, and the hydrological cycle. *Science, 294*, 2119−2124.

Remer, L. A., Kaufman, Y. J., Tanré, D., Mattoo, S., Chu, D. A., Martins, J. V., et al. (2005). The MODIS aerosol algorithm, products and validation. *Journal of the Atmospheric Sciences, 62*(4), 947−973.

Satheesh, S. K., & Ramanathan, V. (2000). Large differences in tropical aerosol forcing at the top of the atmosphere and Earth's surface. *Nature, 405*, 60−63.

Satheesh, S. K., & Srinivasan, J. (2005). A method to infer short wave absorption due to aerosols using satellite remote sensing. *Geophysical Research Letters, ISSN: 0094-8276, 32*(13). doi:10.1029/2005GL023064

Schaaf, C. B., Gao, F., Strahler, A. H., Lucht, W., Li, X., Tsang, T., et al. (2002). First operational BRDF, albedo nadir reflectance products from MODIS. *Remote Sensing of Environment, 83*, 135−148.

Schuster, G., Dubovik, O., Holben, B., & Clothiaux, E. (2005). Inferring black carbon content and specific absorption from Aerosol Robotic Network (AERONET) aerosol retrievals. *Journal of Geophysical Research, ISSN: 0148-0227, 110*(D10). doi:10.1029/2004JD004548

Tanré, D., Haywood, J., Pelon, J., Léon, J. F., Chatenet, B., Formenti, P., et al. (2003). Measurement and modeling of the Saharan dust radiative impact: Overview of the Saharan Dust Experiment (SHADE). *Journal of Geophysical Research, ISSN: 0148-0227, 108*(D18). doi:10.1029/2002JD003273

Torres, O., Bhartia, P. K., Sinyuk, A., Welton, E. J., & Holben, B. (2005). Total Ozone Mapping Spectrometer measurements of aerosol absorption from space: Comparison to SAFARI 2000 ground-based observations. *Journal of Geophysical Research, ISSN: 0148-0227, 110*(D10). doi:10.1029/2004JD004611